JOURNAL OF ENGINEERING SCIENCES

Volume 9, Issue 1 (2022)

Nogueira E. (2022). Thermodynamic performance of boehmite alumina nanoparticle shapes in the counterflow double pipe heat exchanger. Journal of Engineering Sciences, Vol. 9(1), pp. F1-F10, doi: 10.21272/jes.2022.9(1).f1

Thermodynamic Performance of Boehmite Alumina Nanoparticle Shapes in the Counterflow Double Pipe Heat Exchanger

Nogueira E.

Department of Mechanic and Energy, State University of Rio de Janeiro,
R. São Francisco Xavier, 524, Maracanã St., 20550-013, Rio de Janeiro, Brazil

Article info:
Submitted: January 21, 2022
Accepted for publication: March 18, 2022
Available online: March 21, 2022

***Corresponding email:**
elcionogueira@hotmail.com

Abstract. This work compares a theoretical model with a consolidated numerical model related to the thermodynamic performance of boehmite alumina nanoparticles in different formats in a counterflow double pipe heat exchanger. The shapes of the non-spherical nanoparticles under analysis are platelets, blades, cylindrical, and bricks. The second law of thermodynamics is applied to determine Nusselt number, pressure drop, thermal efficiency, thermal and viscous irreversibilities, Bejan number, and the out temperature of the hot fluid. The entropy generation rates associated with the temperature field and the viscous flow are graphical determined. The numerical model uses the k-ε turbulence model, which requires empirical factors to simulate turbulent viscosity and rate of generation of turbulent kinetic energy. Compatibility between the models was demonstrated. It was shown that the maximum absolute numerical error between the quantities Nusselt number, heat transfer rate, and pressure drop for established and specific conditions is less than 12.5 %.

Keywords: energy efficiency, thermal efficiency, Reynolds number, Nusselt number, process innovation.

1 Introduction

The optimization of heat exchangers has become a constant due to the increasing energy demand, and several alternative methods have been proposed. Conventional methods use fin systems, tabulators, and others. However, one of the current methods that have seen remarkable growth involves using fluids with a higher thermal conductivity than usual fluids, metallic or non-metallic solid nanoparticles in base fluids. In addition, recent studies indicate that non-spherical nanoparticles of different shapes can contribute to greater thermal performance than spherical nanoparticles.

The present work aims to compare analytical and numerical models that use the second law of thermodynamics to determine the thermal performance of a double tube heat exchanger. The numerical model, developed by Mostafa Monfared et al. [1], presents results for generating thermal and viscous entropy using nanoparticles of different shapes.

2 Literature Review

Mostafa Monfared et al. [1] numerically analyze the effects of the shape of boehmite alumina nanoparticles on the entropy generation characteristics of a double tube heat exchanger. The non-spherical nanoparticles used in the analysis are of the cylindrical, blade, platelet, and brick type and were dispersed in mixtures of water and ethylene glycol (50%). The entropy generation rates, thermal and frictional, were determined numerically, and the results demonstrated that non-spherical nanoparticles generally provide greater thermal performance than spherical nanoparticles. Furthermore, they conclude that non-spherical platelet-shaped nanoparticles perform better and that the thermal entropy generation rate gives the highest contribution to the total entropy generation rate.

Behrouz Raei and Sayyed Mohsen Peyghambarzadeh [2] experimentally investigated the thermal efficiency of γ-Al_2O_3/water nanofluids using a double tube heat exchanger with nanoparticles dispersed in distilled water at 0.05–0.15 % vol. Experiments were carried out under a turbulent flow regime ($1.8 \cdot 10^4 < Re < 4 \cdot 10^4$) and

nanofluid inlet temperatures ranging from 45 °C to 65 °C. The results obtained in the study showed that the addition of nanoparticles to the base fluid increases the heat transfer rate by up to 16 %. Furthermore, they find that the thermal performance factor of this nanofluid reaches 1.1 for a concentration of 0.15 % vol. and a Reynolds number equal to 18,000.

Salah Almurtaji et al. [3] present a work that provides a review of the technology used in heat exchangers and analyzes how nanofluids can improve thermo-hydraulic performance. In addition, they discuss the nanofluid development process and emphasize the role of nanoparticles as fundamental elements to increase the thermal efficiency of heat exchangers in future applications.

Xiao Feng Zhou and L. Gao [4] uses the effective differential medium theory, considering the interfacial thermal resistance between solid particles and the host medium, to determine the effective thermal conductivity in nanofluids of non-spherical solid particles. They report an increase in the effective thermal conductivity of non-spherical nanoparticles. Furthermore, they draw attention to the fact that the increase in interfacial thermal resistance between the media causes degradation in the rise in thermal conductivity. The theoretical and experimental results show the non-linear dependence of the effective thermal conductivity on the volume fractions of non-spherical nanoparticles.

Elena V. Timofeeva et al. [5] experimentally evaluate the efficiency of nanofluids and the relationship between thermal conductivity and viscosity. They investigate and model thermal conductivity and viscosity in a fluid consisting of equal ethylene glycol and water volumes. They note that thermal conductivity is affected due to interfacial interactions proportional to the surface area of the nanoparticles and that this also plays a crucial role in determining viscosity. They demonstrate that nanofluid viscosity can be reduced by adjusting the pH of the nanofluid without affecting thermal conductivity.

Máté Petrik et al. [6] carry out studies to numerically investigate the heat transfer in a double tube heat exchanger. They find that there are constructions of heat exchangers capable of transferring the specified heat transfer rate. Still, only one geometry has a lower cost for the material type, inside and outside diameters, and tube length. They find that the thermodynamic performance of the heat exchanger strongly depends on the geometry. They show that the configuration that allows for the highest version can be determined from the initial conditions when specified flow rates and outlet temperatures.

Hamid Shamsabadi et al. [7] perform a numerical simulation to investigate thermal and viscous irreversibilities for Al_2O_3-nanofluid in a pipeline with porous baffles. The Reynolds number, the nanoparticles volume fraction, the number of baffles, and the Darcy number were used to determine the thermal and viscous entropy generation rates and the Bejan number. They determined that the viscous and thermal entropy generation rates decrease with the increasing number of baffles for $N > 4$ and that the reductions are equal to 14 % and 32 %, respectively. In addition, they find that thermal entropy generation is dominant, except in the space between the lower and upper deflectors where the velocity gradients are high.

Adrian Bejan [8] published during the 1980s a review on the application of the second law of thermodynamics with emphasis on aspects related to the entropy generation rate. He discussed relevant aspects related to thermal irreversibility and viscous irreversibility. The most pertinent part of the review highlights how reducing irreversibilities at the component level affects the entire system.

Ahmad Fakheri [9] presents effectiveness as the ratio between the current heat transfer rate and the ideal heat transfer rate, based on the second law of thermodynamics. It defines efficiency as a function of a single dimensionless parameter called the fin analogy. It shows how efficiency and irreversibility defined based on the second law of thermodynamics provide a new avenue for designing and analyzing heat exchangers. It determines expressions for efficiency to be applied to parallel flow, counterflow, and cross-flow heat exchangers. The approach based on the second law of thermodynamics makes the performance analysis of heat exchangers simpler and more elegant. Nogueira E. [10; 11] uses this new way for studying heat exchangers.

Nogueira E. [10] applies the second law of thermodynamics in a shell and tube heat exchanger. Water-ethylene glycol associated with volume fractions of nanoparticles flows in the tube and water flows in the shell. Nanofluids of Ag and Al_2O_3 enters the reservoir at 90 ºC and water at 27 ºC. The volume fractions of nanoparticles are equal to 0.01, 0.10, and 0.25. It is demonstrated that using the second law and efficiency, effectiveness, and irreversibility concepts, the thermal performance of the heat exchanger is strongly affected by the flow regime.

Nogueira E [11] uses the second law and concepts of efficiency and effectiveness to determine the heat transfer rate in a shell and helical coil tube heat exchanger where the water is heated. The objective of the work is to determine the heat transfer rate that satisfies the imposed conditions for heating the solution of water and ammonium nitrate (ANSOL) without crystallization. The Reynolds number, the Nusselt number, and the global heat transfer coefficient are the intermediate quantities needed to reach the objective.

3 Research Methodology

Ethylene glycol flows in the inner tube with dispersed non-spherical Boehmite Alumina nanoparticle fractions. Hot water flows in the annular region opposite the nanofluid. The hot fluid enters the outer tube at a uniform temperature equal to 35 °C. The nanofluid enters the inner tube at a uniform temperature equal to 25°C. The Reynolds number associated with the hot fluid is fixed and equal to 10,000. The Reynolds number associated with the nanofluid varies from 10,000 to 20,000. The

volume fractions of nanoparticles vary between 0.005 and 0.020, from 0.5 % to 2.0 %. Figure 1 schematically represents the counterflow double pipe heat exchanger. Table 1 presents the thermodynamic property values for water, ethylene glycol, and the spherical nanoparticles of Boehmite Alumina. The length of the tube is equal to 1.5 m, and the diameters of the inner and outer tubes are 8.83 mm and 30.85 mm, respectively.

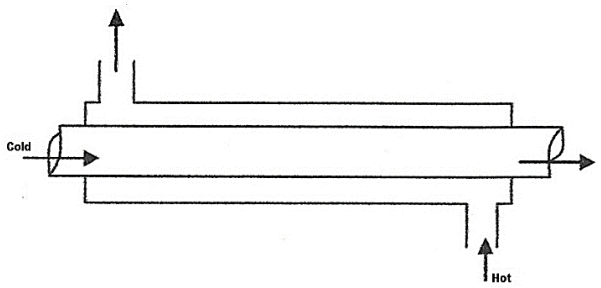

Figure 1 – The design scheme of a counterflow double pipe heat exchanger

Table 1 – Hot (water), cold (ethylene glycol 50 %) fluids and nanoparticles properties

Param.	ρ, $\frac{kg}{m^3}$	k, $\frac{W}{m \cdot K}$	C_p, $\frac{J}{kg \cdot K}$	μ, 10^{-3} $\frac{kg}{m \cdot s}$	v, 10^{-6} m/s^2	α, 10^{-6} m/s^2
Hot	994	0.623	4178	0.72	0.724	0.150
Cold	1067	0.38	3300	3.39	24.045	0.108
Al_2O_3	3950	31.9	873	–	–	9.250
B alum.	3050	30	618	–	–	15.90

Table 2 below was included in the numerical article published by Mostafa Monfared et al. [1] and presented coefficients that characterize non-spherical nanoparticles concerning dynamic and thermal aspects. The coefficient C_k characterizes the thermal conductivity, and the coefficients A_1 and A_2 characterize the dynamic viscosity. These coefficients are used in the present analytical model.

Table 2 – Coefficients that characterize the non-spherical shape of nanoparticles in dynamic viscosity and thermal conductivity [1]

Type	C_k	A_1	A_2
Platelets	2.61	37.1	612.6
Blades	2.74	14,6	123.3
Cylindrical	3.95	13.5	904.4
Bricks	3.37	1.9	471.4

The properties of the nanofluids are given by:

$$\rho_{nano} = \rho_{Particle}\,\phi + (1-\phi)\,\rho_C; \quad (1)$$

$$\mu_{nano} = \frac{\mu_C}{(1-\phi)^{2.5}}; \quad (2)$$

$$\mu_{nano} = \mu_C\,(1 + A_1\,\phi + A_2\phi^2)\;for\;non - spherical\;shape; \quad (3)$$

$$Cp_{nano} = \frac{Cp_{Particle}\,\rho_{Particle}\,\phi + (1-\phi)\,Cp_C\,\rho_C}{\rho_{nano}}; \quad (4)$$

$$k_{nano} = \left[\frac{[k_{Particle}+2\,k_C+2\,(k_{Particle}-k_C)\,(1-0.1)^3\,\phi]}{[k_{Particle}+2\,k_C+2\,(k_{Particle}-k_C)\,(1-0.1)^2\,\phi)]}\right] K_C; \quad (5)$$

$$k_{nano} = k_C\,(1 + C_k\,\phi)\;for\;non - spherical\;shape; \quad (6)$$

$$\nu_{nano} = \frac{\mu_{nano}}{\rho_{nano}}; \quad (7)$$

$$\alpha_{nano} = \frac{k_{nano}}{\rho_{nano}\,Cp_{nano}}; \quad (8)$$

$$Pr_{nano} = \frac{\mu_{nano}}{\alpha_{nano}}, \quad (9)$$

where ϕ – the nanoparticle volume fraction;

$$Nu_{nano} = \frac{\left(\frac{f}{8}\right)(\mathrm{Re}_{nano} - 1000)\,\mathrm{Pr}_{nano}}{1 + 12.7\left(\frac{f}{8}\right)^{\frac{1}{2}}\left(Pr^{\frac{2}{3}} - 1\right)}; \quad (10)$$

where Nu_{nano} – the Nusselt number for the nanofluid. Equation (10) is provided by Gnielinski [12]:

$$f = (0.79\,lnRe_{nano} - 1.64)^{-2}; \quad (11)$$

$$h_{nano} = \frac{Nu_{nano}\,K_{nano}}{D_C}, \quad (12)$$

where h_{nano} – the convective heat transfer coefficient, and D_C is the inner diameter;

$$Nu_h = 0.023\,{Re_h}^{0.8}\,{Pr_h}^{0.4}; \quad (13)$$

$$h_h = \frac{Nu_h \cdot k_h}{Dh_h}; \quad (14)$$

$$Dh_h = D_h - D_c, \quad (15)$$

where Nu_h, h_h, and Dh_h – the Nusselt number, convective heat transfer coefficient, and hydraulic diameter for the hot fluid; D_h – the out diameter;

$$As_C = \pi\,D_C\,L_{DPHE}; \quad (16)$$

$$As_h = \pi\,Dh_h\,L_{DPHE}, \quad (17)$$

where As_C and As_h – the superficial areas of heat exchange; L_{DPHE} – the length of the double pipe heat exchanger;

$$Nu_{Med} = \frac{Nu_{nano} + Nu_h}{2}; \quad (18)$$

$$h_{Med} = Nu_{Med}\left(\frac{K_{nano}}{D_C}\right) \quad (19)$$

$$A_{Med} = \frac{As_h + As_C}{2}; \quad (20)$$

$$Uo = \frac{1}{\frac{1}{h_{Med}}}, \quad (21)$$

where Uo – the global convective heat transfer coefficient;

$$Ac_C = \frac{\pi\, {D_C}^2}{4}; \quad (22)$$

$$Ac_h = \frac{\pi\, {Dh_h}^2}{4}; \quad (23)$$

where Ac_C and Ac_h – the cross-sectional areas of the inner and outer tubes, respectively;

$$\dot{m}_h = \frac{Re_h\, \mu_h\, Ac_h}{Dh_h}; \quad (24)$$

$$\dot{m}_C = \frac{Re_{nano}\, \mu_{nano}\, Ac_C}{D_C}; \quad (25)$$

where $\dot{m}_h$ and $\dot{m}_C$ – the mass flow rate of hot and cold fluid, respectively;

$$C_h = \dot{m}_h\, Cp_h; \quad (26)$$

$$C_{nano} = \dot{m}_C\, Cp_{nano}; \quad (27)$$

where C_h and C_{nano} – heat capacity of hot and nanofluid, respectively;

$$C^* = \frac{C_{min}}{C_{max}}; \quad (28)$$

$$NTU = \frac{Uo\, A_{Med}}{C_{min}}; \quad (29)$$

where NTU is the number of the transfer unit;

$$Fa = \left(\frac{NTU}{2}\right)(1 - C^*), \quad (30)$$

where Fa – the nondimensional fin analogy number for the counterflow heat exchanger;

$$\eta_T = \frac{tanh(Fa)}{Fa}; \quad (31)$$

$$\varepsilon_T = \frac{1}{\frac{1}{\eta_T\, \mathrm{NTU}} + \frac{1 + \mathrm{C}^*}{2}}; \quad (32)$$

where η_T – the thermal efficiency; ε_T – the effectiveness;

$$\dot{Q} = (Th_i - Tc_i)\, C_{min}\, \varepsilon_T; \quad (33)$$

$$\dot{Q}_{max} = (Th_i - Tc_i)\, C_{min}; \quad (34)$$

where $\dot{Q}$ – the heat transfer rate;

$$Th_o = Th_i - \frac{\dot{Q}}{\dot{m}_h\, Cp_h}; \quad (35)$$

$$Tc_o = Tc_i + \frac{\dot{Q}}{\dot{m}_c\, Cp_{nano}}; \quad (36)$$

$$\sigma_T = \left(\frac{C_h}{C_{min}}\right) ln\left(\frac{Th_o}{Th_i}\right) + \left(\frac{C_{nano}}{C_{min}}\right) ln\left(\frac{Tc_o}{Tc_i}\right); \quad (37)$$

where σ_T – the thermal irreversibility;

$$\dot{S}_{Tgen} = \sigma_T\, C_{min}; \quad (38)$$

where $\dot{S}_{Tgen}$ – the thermal entropy generation rate;

$$V_C = \frac{\dot{m}_C}{\rho_{nano}\, Ac_C}; \quad (39)$$

$$V_h = \frac{\dot{m}_h}{\rho_{nano}\, Ac_h}; \quad (40)$$

$$f_C = \frac{0.316}{{Re_{nano}}^{0.25}}; \quad (41)$$

$$f_h = \frac{0.316}{{Re_h}^{0.25}}; \quad (42)$$

where f_C and f_h – the friction factors for cold and hot fluids, respectively;

$$\Delta P_C = \frac{f_C\, \left(\frac{L_{DPHE}}{D_C}\right) \rho_{nano}\, {V_C}^2}{2}; \quad (43)$$

$$\Delta P_h = \frac{f_h\, \left(\frac{L_{DPHE}}{Dh_h}\right) \rho_h\, {V_h}^2}{2}; \quad (44)$$

where ΔP_h and ΔP_C – the pressure drops for hot and cold fluids, respectively;

$$Pc_2 = Ph_2 = Patm; \quad (45)$$

where $Pc_2\ and\ Ph_2$ – the outlet pressures (according to the hypothesis).

Then:

$$Pc_1 = Pc_2 + \Delta P_C; \quad (46)$$

$$Ph_1 = Ph_2 + \Delta P_h; \quad (47)$$

$$Pc_{21} = \frac{Pc_2}{Pc_1}; \quad (48)$$

$$Ph_{21} = \frac{Ph_2}{Ph_1}; \quad (49)$$

$$R = \frac{Th_i - Th_o}{Tc_o - Tc_i}; \quad (50)$$

$$\sigma_f = \left(\frac{C_h}{C_{min}}\right) ln(Ph_{21}) + \left(\frac{C_{nano}}{C_{min}}\right) R\, ln(Pc_{21}); \quad (51)$$

$$\dot{S}_{fgen} = \sigma_f \, C_{min}; \tag{52}$$

where σ_f and $\dot{S}_{fgen}$ – the viscous irreversibility and the viscous entropy generation rate;

Finally, we have:

$$Be = \frac{\dot{S}_{Tgen}}{\dot{S}_{Tgen} + \dot{S}_{fgen}}, \tag{53}$$

where Be – the Bejan thermodynamic number.

4 Results and Discussion

Figure 2 shows values for the Nusselt number as a function of the Reynolds number of the nanofluid for a volume fraction rate equal to 2.0 %.

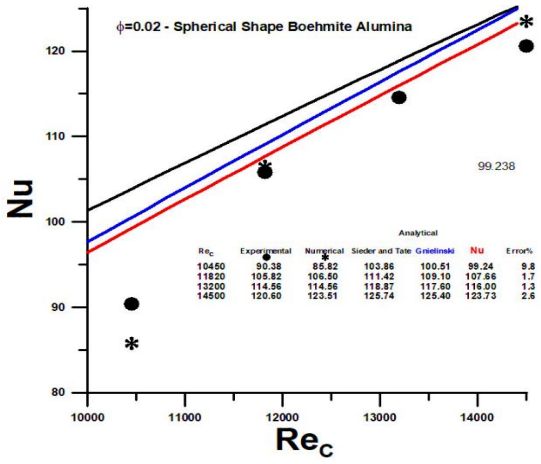

Figure 2 – Nusselt number vs. Reynolds number for Spherical Boehmite Alumina

The equations used to determine the Nusselt number for the nanofluid were independently determined by Sieder, Tate, and Gnielisnki. The highlight in red shows results for the Nusselt number used in work, resulting from the average of the Nusselt numbers in both media. When compared with experimental results presented in [1], the absolute error is less than 10 % within the range of Reynolds number values under analysis. For high Reynolds numbers, the values show better precision.

Figures 3, 4 show values for Nusselt number as a function of Reynolds number for 0.5 % and 2.0 % of nanoparticles fraction. The performance of non-spherical platelet nanoparticles and the low performance for the spherical particle Boehmite Alumina stands out. The results of Boehmite Alumina are inferior to Ethylene Glycol.

Nusselt number as a function of the volume fraction for the Reynolds number of the nanofluid equal to 10,000 is shown in Figure 5. The Nusselt number increases with the addition of the volume fraction for all non-spherical nanoparticles. Conversely, the spherical particles decrease the Nusselt number, emphasizing Boehmite Alumina, which presents values lower than Ethylene Glycol.

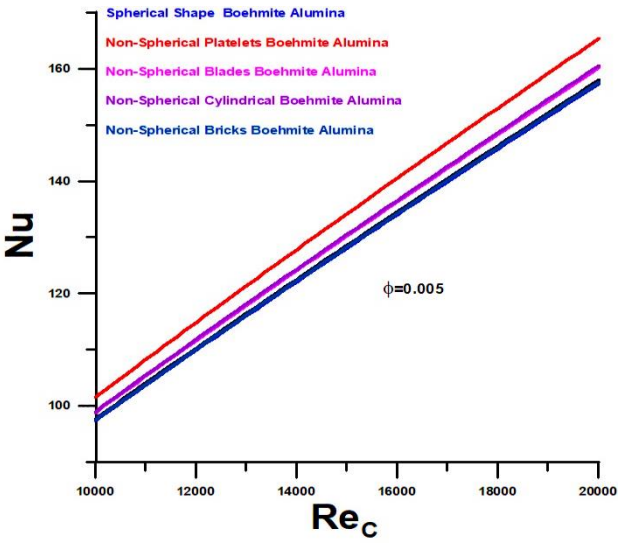

Figura 3 – Nusselt number vs. Reynolds number for the volume fraction of 0.5 % vol.

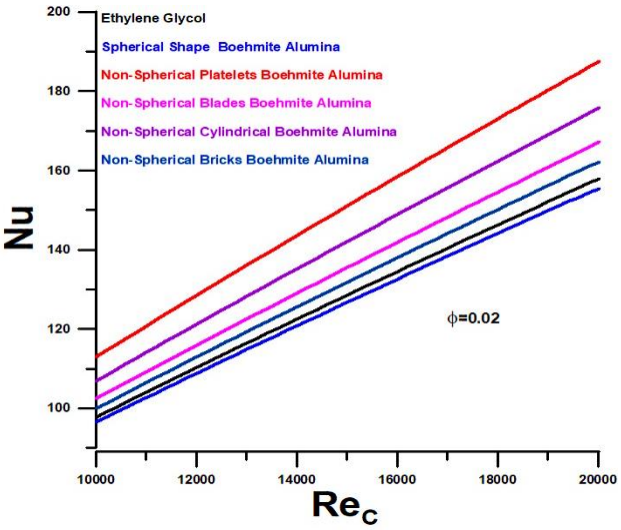

Figura 4 – Nusselt number vs. Reynolds number for the volume fraction of 2.0 % vol.

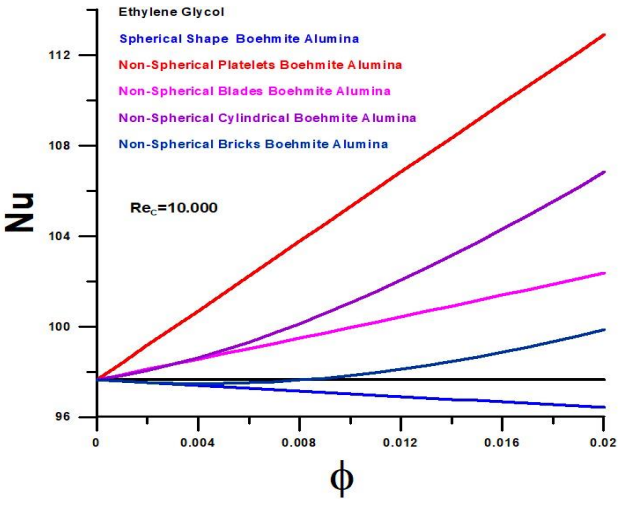

Figure 5 – Nusselt number vs. volume fraction for Re_c = 10,000

The highest value obtained for the Nusselt Number is associated with platelet nanoparticles, followed by cylindrical, blades and bricks. The numbers obtained for the Nusselt number with Re_c = 20,000 are higher than those obtained for Re_c = 10,000, as shown in Figure 6. The observed trend remains the same concerning the nanoparticles under analysis.

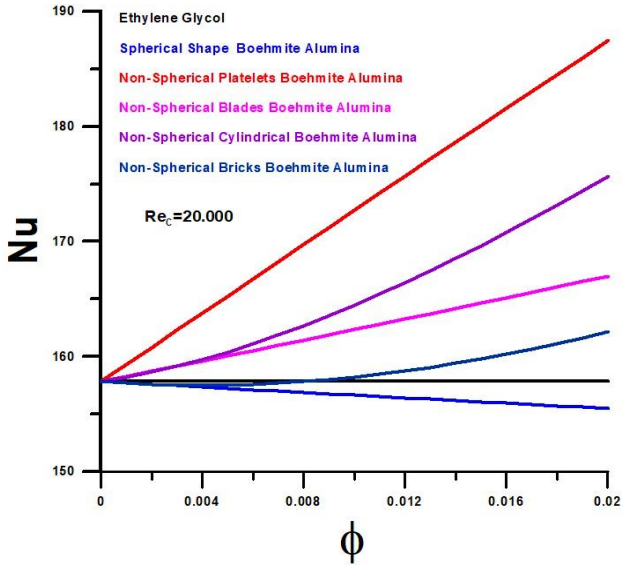

Figure 6 – Nusselt number vs. volume fraction for Re_c = 20,000

As a function of the volume fraction, values for heat transfer rate are shown in Figure 7.

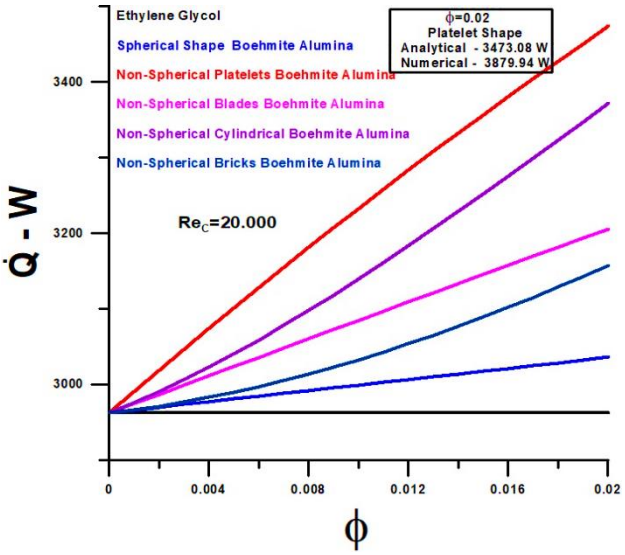

Figure 7 – Heat transfer rate vs. volume fraction for Re_c = 20,000

The thermal performance presented for non-spherical nanoparticles is equivalent to that already observed. However, it is worth noting that the spherical nanoparticle of Boehmite Alumina has a higher heat transfer rate than Ethylene Glycol for the entire volume fraction range under analysis.

In the highlight, a comparison between the analytical and numerical models is presented, with values taken from the reference [1], with an absolute percentage error equal to 10.5 %.

Pressure drop as a function of volume fraction, with Re_c = 20,000, is shown in Figure 8.

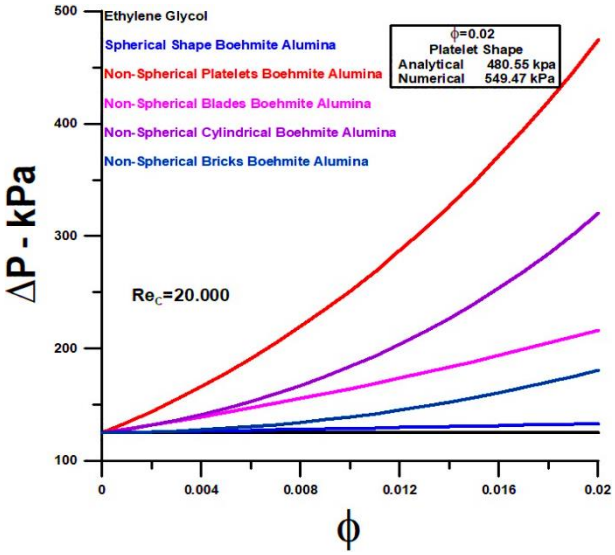

Figure 8 – Pressure drop vs. volume fraction with Re_c = 20,000

Pressure drop increases with volume fraction for all nanoparticles. The highest value obtained for the pressure drop is associated with platelet nanoparticles, followed by cylindrical, blades, bricks, and spherical nanoparticles, equivalent to the Nusselt number. In the highlight, a comparison between the analytical and numerical models is presented, with values taken from the reference [1], with an absolute percentage error equal to 12.5%.

Figure 9 presents results for thermal efficiency as a function of nanoparticles volume fraction for the highest Reynolds number under analysis, i.e., Re_c = 20,000.

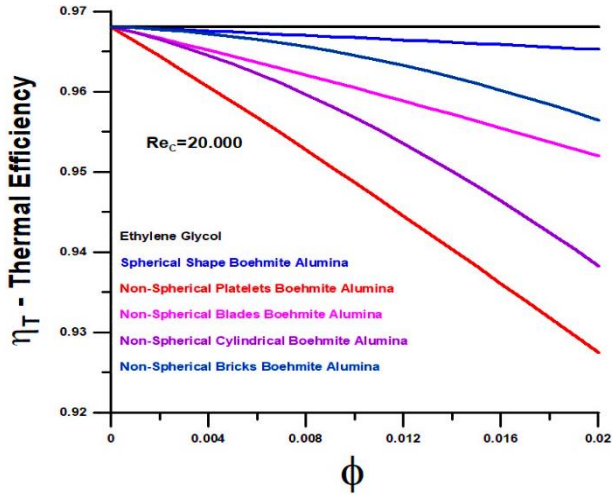

Figure 9 – Thermal efficiency vs. volume fraction for Re_c = 20,000

Thermal efficiency decreases with increasing volume fraction for all nanoparticles, with a lower value for the nanoparticle that has greater value for the heat transfer rate for non-spherical platelet nanoparticles. However, the thermal efficiency is high in all situations, with a value close to 1 for ethylene glycol. As a partial conclusion, it can be anticipated that there are conditions to increase the Reynolds number or the volume fraction for all nanoparticles.

Thermal irreversibility appears in Figure 10 and shows the opposite trend to thermal efficiency, increasing where efficiency decreases.

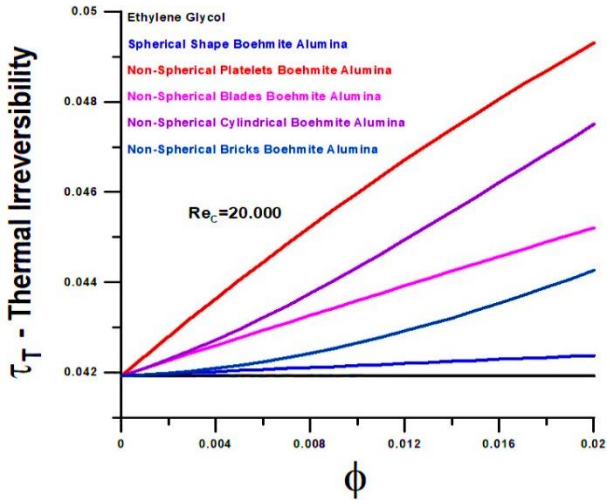

Figure 10 – Thermal irreversibility vs. volume fraction with Re_c = 20,000

However, the irreversibility is significantly low, demonstrating, once again, that there is an enormous possibility of increasing the Reynolds number, or the volume fraction of nanoparticles, to achieve greater thermal performance for the heat exchanger in question.

Figure 11 presents results for viscous irreversibility as a function of volume fraction for the highest Reynolds number under analysis, i.e., Re_c = 20,000.

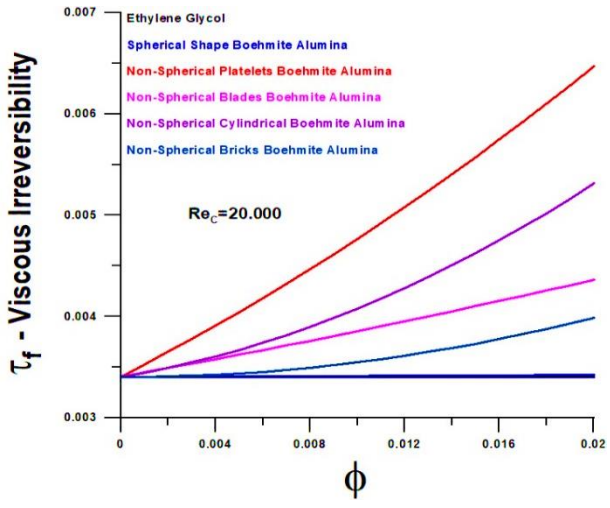

Figure 11 – Viscous irreversibility vs. volume fraction for Re_c = 20,000

Viscous irreversibility increases with the volume fraction for all nanoparticles and presents shallow values in all situations under investigation, with an order of magnitude lower than thermal irreversibility.

Figures 12, 13 show thermal entropy generation rate values as a function of Reynolds number, Re_c = 20,000, and volume fractions of 0.5 % and 2.0 %.

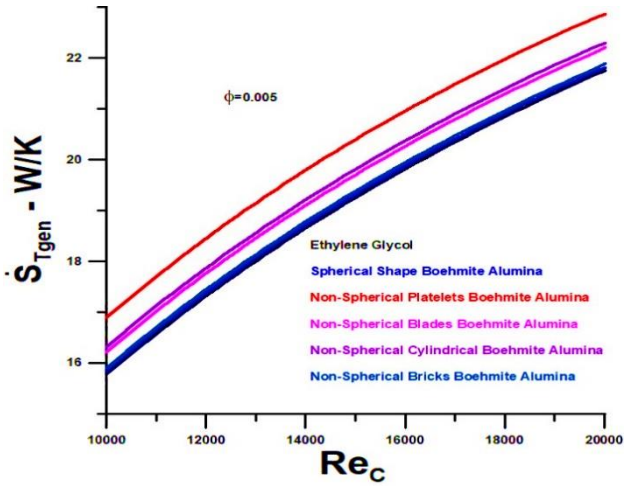

Figure 12 – Thermal entropy generation rate vs. Reynolds number and volume fraction of 0.5 %

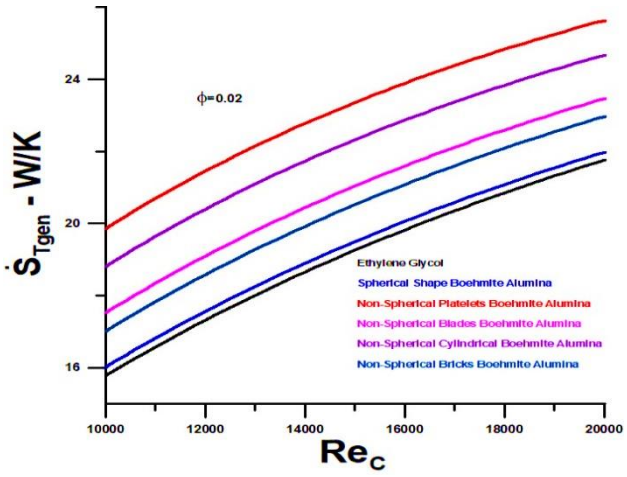

Figure 13 – Thermal entropy generation rate vs. Reynolds number and volume fraction of 2.0 %

Again, the high performance of non-spherical platelet nanoparticles and the low performance for the spherical particle Boehmite Alumina stands out.

Thermal entropy generation rate as a function of volume fraction, for Re_c = 20,000, is shown in Figure 14. The results presented are like those already offered through thermal irreversibility, varying in absolute terms as a function of the minimum thermal capacity under analysis.

The viscous entropy generation rate is shown in Figure 15 and shows values approximately ten times smaller than the thermal entropy rate. The entropy generation rates show higher results for the non-spherical

platelet nanoparticle, followed by the cylindrical, blade, bricks, and spherical Boehmite alumina.

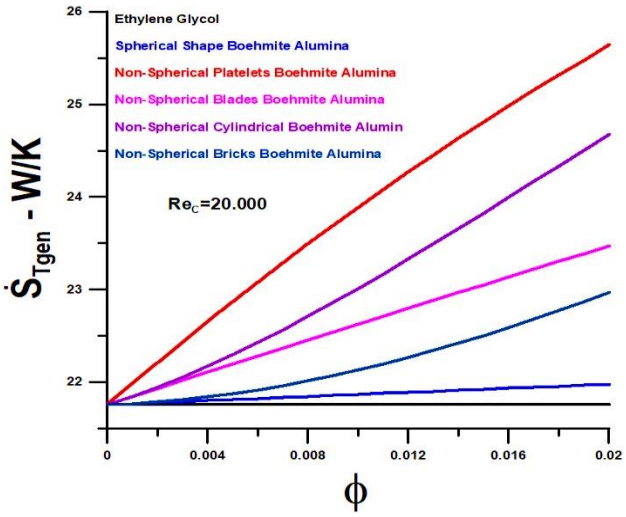

Figure 14 – Thermal entropy generation rate vs. volume fraction for Re_c = 20,000

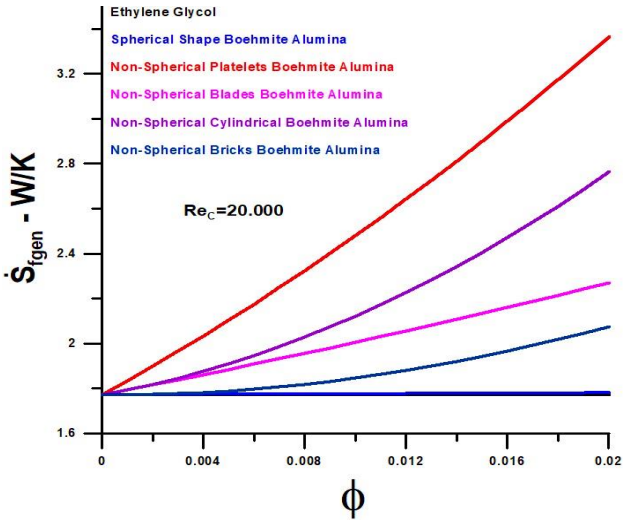

Figure 15 – Viscous entropy generation rate vs. volume fraction for Re_c = 20,000

Figure 16 shows the relationship between thermal entropy generation rates and the total entropy generation rate, represented by the thermodynamic Bejan number. The results show that the rate of thermal entropy generation is prevalent, with very high values, close to 1, with a tendency to fall for non-spherical nanoparticles as the volume fraction increases – a highlight for non-spherical platelet particles. A similar result is demonstrated for thermal efficiency, as already discussed, where non-spherical platelet particle has minor efficiency compared with the others.

Figures 17, 18 show exit temperatures for the hot fluid as a function of the Reynolds number. The outlet temperature decreases with increasing Reynolds number. The non-spherical platelet nanoparticle has lower exit temperatures compared to other nanoparticles. When the nanoparticle volume fraction is greater than 2.0 %, the exit temperature is lower than the volume fraction of 5.0 %.

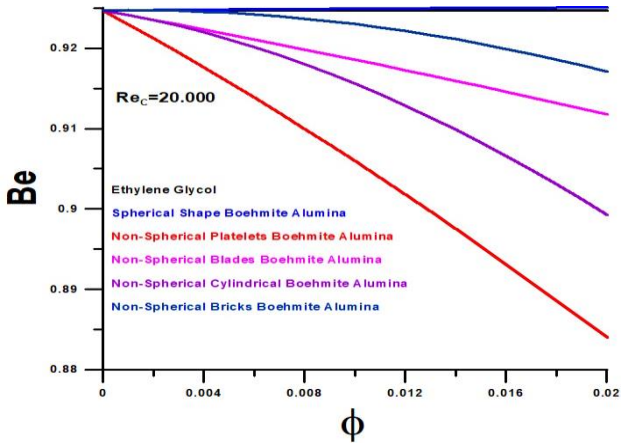

Figure 16 – Bejan vs. volume fraction for Re_c = 20,000

Figure 19 shows the exit temperature as a function of the volume fraction for Reynolds equal to 20,000. The exit temperature decreases with the addition of the Reynolds number.

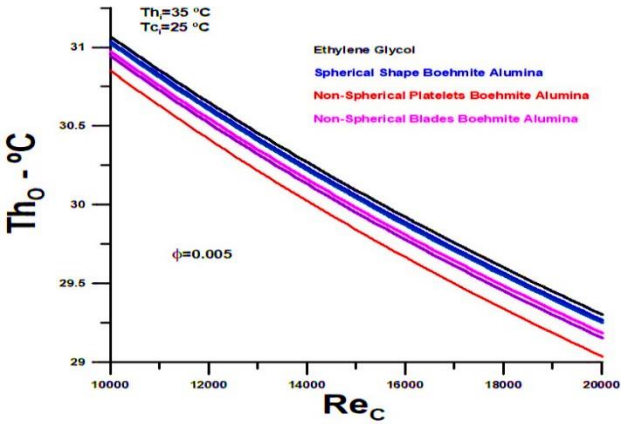

Figure 17 – Hot outlet temperature vs. Reynolds number for the volume fraction of 0.5 %

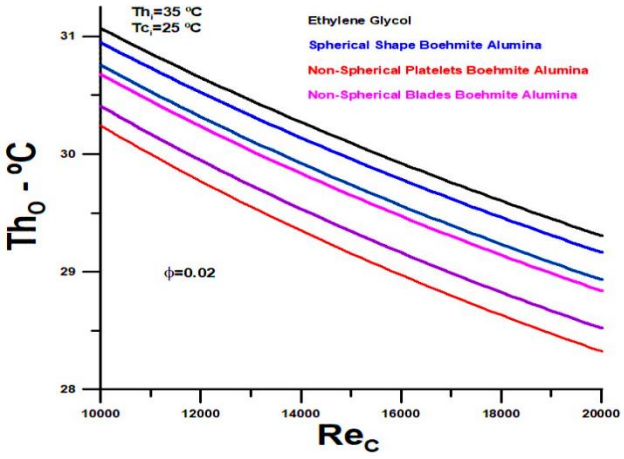

Figure 18 – Hot outlet temperature vs. Reynolds number for the volume fraction of 2.0 %

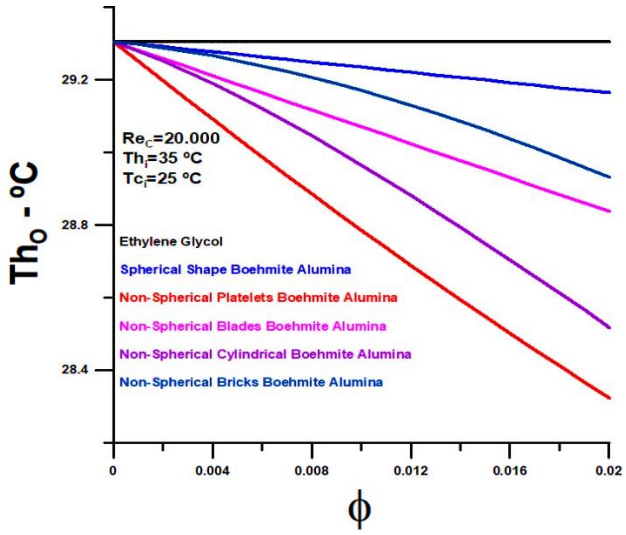

Figure 19 – Hot outlet temperature vs. volume fraction for Re_c = 20,000

The results presented in Figures 17–19 demonstrate, once again, that the heat exchanger has the potential to increase thermal performance, with an increase in Reynolds numbers in both fluids and, or an increase in the percentage of nanoparticles.

Therefore, it is added, for analysis, an expansion for the Reynolds number and the volume fraction, as shown in Figures 20, 21. In these cases, the platelet nanoparticle is considered for analysis since it has better thermal performance.

The heat transfer rate for the non-spherical platelet nanoparticle, with Reynolds number magnification to 40,000 and volume fraction to 8.0 %, asymptotically approximates the maximum exchange possible with the current heat exchanger configuration.

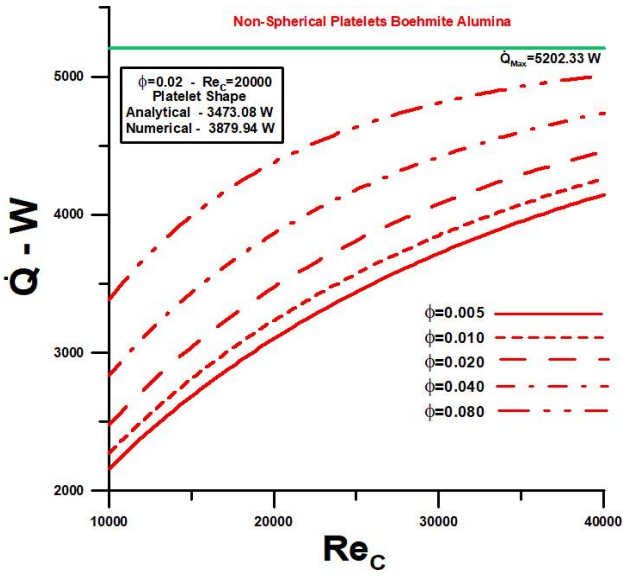

Figure 20 – Heat transfer rate actual and maximum vs. Reynolds number with volume fractions

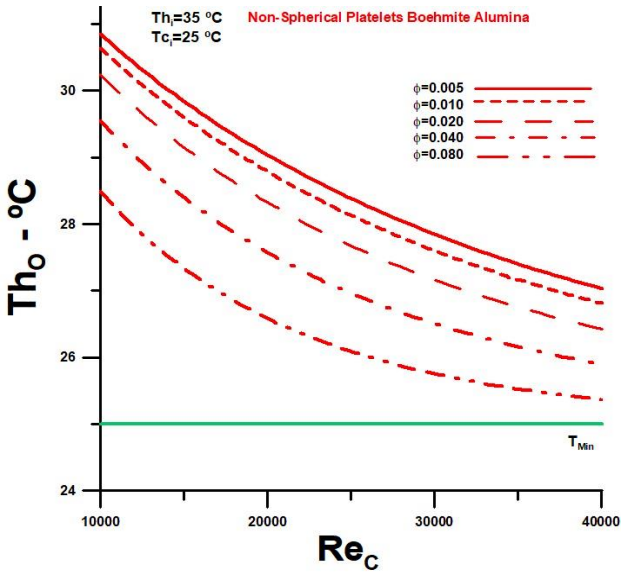

Figure 21 – Outlet hot temperature actual and minimum vs. Reynolds number with volume fractions

The exit temperature for the non-spherical platelet nanoparticle, with Reynolds number magnification to 40,000 and volume fraction to 8.0 %, asymptotically approximate the minimum possible temperature for the current heat exchanger configuration.

The latest results presented in Figures 20, 21 consolidate the conclusions previously presented in this work, and demonstrate that non-spherical nanoparticles, especially platelet nanoparticles, have great potential to improve the thermal performance of heat exchangers in general.

5 Conclusions

Non-spherical nanoparticles dispersed in a mixture of water and ethylene glycol (50 %) were used in an analytical study counterflow double pipe heat exchanger, applying the second law of thermodynamics.

The effect of nanoparticle shapes on the thermodynamic performance of the heat exchanger was analyzed. The analyzed nanoparticles were spherical Boehmite Alumina nanoparticles and non-spherical Boehmite Alumina nanoparticles of platelets, cylindrical, blades, and bricks.

The results of the analytical study were compared with numerical and experimental results presented in the literature regarding the Nusselt number, heat transfer rate, and pressure drop and given maximum absolute error equal to 12.5 %.

The main conclusions of the work are as follows. Firstly, non-spherical nanoparticles have better thermal performance than ethylene glycol (50 %) and spherical nanoparticles.

Secondly, the highlight regarding thermal performance is for non-spherical platelet nanoparticles.

Thirdly, thermal efficiency drops with the volume fraction of nanoparticles. Also, thermal irreversibility increases with the volume fraction of nanoparticles.

Additionally, the relationship between the thermal entropy generation rate and the total entropy generation rate, represented by the Bejan number, is relatively high.

Finally, the analyzed heat exchanger presents better thermal performance with an increase in the Reynolds number in both fluids and an increase in the volume fraction of the nanoparticles concerning what was studied numerically.

References

1. Monfared, M., Shahsavar, A., Bahrebar, M. R. (2019). Second law analysis of turbulent convection flow of boehmite alumina nanofluid inside a double-pipe heat exchanger considering various shapes for nanoparticle. *Journal of Thermal Analysis and Calorimetry*, Vol. 135, pp. 1521-1532, doi: 10.1007/s10973-018-7708.
2. Raei, B., Peyghambarzadeh, S. M. (2019). Measurement of local convective heat transfer coefficient of alumina-water nanofluids in a double tube heat exchanger. *Journal of Chemical and Petroleum Engineering*, Vol. 53(1), pp. 25-36, doi: 10.22059/jchpe.2019.265521.1247.
3. Almurtaji, S., Ali, N., Teixeira, J. A., Addali, A. (2020). On the role of nanofluids in thermal-hydraulic performance of heat exchangers – A review. *Nanomaterials*, Vol. 10, 734, doi: 10.3390/nano10040734.
4. Zhou, X. F., Gao, L. (2006). Effective thermal conductivity in nanofluids of non-spherical particles with interfacial thermal resistance: Differential effective medium theory. *Journal of Applied Physics*, Vol. 100, 024913, doi: 10.1063/1.2216874.
5. Timofeeva, E. V., Routbort, J. L., Singh, D. (2009). Particle shape effects on thermophysical properties of alumina nanofluids. *Journal of Applied Physics*, Vol. 106, 014304, doi: 10.1063/1.3155999.
6. Petrik, M., Szepesi, G., Jármai, K. (2018). Optimal design of double-pipe heat exchangers. *Advances in Structural and Multidisciplinary Optimization*, pp. 755-764, doi: 10.1007/978-3-319-67988-4_57.
7. Shamsabadi, H., Rashidi, S., Esfah, J. A. (2018). Entropy generation analysis for nanofluid flow inside a duct equipped with porous baffles. *Journal of Thermal Analysis and Calorimetry*, Vol. 135, pp. 1009-1019, doi: 10.1007/s10973-018-7350-4.
8. Bejan, A. (1987). The thermodynamic design of heat and mass transfer processes and devices. *Heat and Fluid Flow*, Vol. 8(4), pp. 258-276.
9. Fakheri, A. (2007). Heat exchanger efficiency. *Transactions of the ASME*, Vol. 129, pp. 1268-1276, doi: 10.1016/j.applthermaleng.2017.05.076.
10. Nogueira, E. (2020). Thermal performance in heat exchangers by the irreversibility, effectiveness, and efficiency concepts using nanofluids. *Journal of Engineering Sciences*, Vol. 7, pp. F1-F7, doi: 10.21272/jes.2020.7(2).f1.
11. Nogueira, E. (2021). Efficiency and effectiveness thermal analysis of the shell and helical coil tube heat exchanger used in an aqueous solution of ammonium nitrate solubility (ANSOL) with 20% H_2O and 80% AN. *Journal of Materials Science and Chemical Engineering*, Vol. 9, pp. 24-45, doi: 10.4236/msce.2021.96003.
12. Gnielinski, V. (1976). New equations for heat and mass transfer in turbulent pipe and channel flow. *International Chemical Engineering*, Vol. 16(2), pp. 359-68.